Ion Selectivity of a Biological Channel at High Concentration Ratio: Insights on Small Ion Diffusion and Binding

M. Lidón López, Marcel Aguilella-Arzo, Vicente M. Aguilella, and Antonio Alcaraz*

Department of Physics, Laboratory of Molecular Biophysics, University Jaume I, Av. Sos Baynat, s/n, 12080 Castellón, Spain

Received: March 13, 2009; Revised Manuscript Received: April 23, 2009

The ionic selectivity of the bacterial porin OmpF has been investigated in several chloride salts of alkali metal cations under a wide range of concentration ratios. We report a novel way of studying the several factors contributing to ionic selectivity of large channels: measuring reversal potential beyond the gradients commonly used in channel selectivity experiments, i.e., over 50-fold salt concentration ratios. Our results reveal an additional channel feature slipped by in previous studies: the interaction of mobile ions with the protein channel transforms noticeably the ion intrinsic diffusivities. The cation/anion diffusivity ratios in the channel are approximately half of their bulk values for all alkali metal cations studied (KCl, NaCl, LiCl, and CsCl). The binding of cations to certain acidic channel residues is likely to be involved, and its contribution is essential to account for the observed traits. A simple molecular model based on statistical thermodynamics provides qualitative explanations to the experimental findings and can be useful for future, more elaborated treatments.

Introduction

Ion selectivity is an essential property of a number of synthetic and biological nanopores. Among the latter group, protein channels are probably the most extensively studied because of their physiological function in cells regulating the transport of charged and neutral solutes and generating electromotive forces required for electrical signaling.[1] One could imagine that there is a unique common pattern in the physicochemical basis of ion transport across such objects. However, even within the nanoscale, a manifest contrast can be found between the selective properties of narrow channels, specifically designed to allow transport of specific solutes, and the selectivity of large channels, which usually exhibit multiionic transport as well as permeation of metabolites between cells and organelles within cells.[2,3]

Over the last years, we have conducted a number of experimental and theoretical studies[4−10] aimed to understand the physicochemical mechanisms of small ion conduction in a large protein channel, the bacterial porin OmpF, which forms wide pores in the outer membrane of *Escherichia coli*.[11,12] The topic is still a matter of debate, since macroscopic descriptions cannot easily anticipate the behavior of water and ions confined at the molecular nanoscale and powerful tools like molecular dynamics rely on atomic structural information that is not always available.[13−16]

There is some generalized consensus about the fact that the selectivity of large channels includes two components: partitioning, an equilibrium measure of the exclusion or accumulation of ions in the channel, and diffusion, a nonequilibrium averaged measure of the relative mobility of ions in the channel.[1,4,17] It is also admitted that, among the physical descriptions of ion channel selectivity, the measurement of reversal potential (RP, the potential needed to get zero current under a concentration gradient) is the method of choice to account for both components of selectivity.[9,18]

Previous studies performed on planar lipid membranes at the single-channel level showed that the OmpF cationic selectivity reported under physiological conditions[16,19] is in fact a strong function of certain parameters like the solution pH and the absolute electrolyte concentration, whereas its dependence on the lipid composition and the direction of the concentration gradient is less significant but still measurable.[4] Those results challenged the classical view of selectivity as an intrinsic feature of the channel and opened new possibilities to tune the rectification properties of the pore[5] and even obtain a directional selectivity: Under certain pH conditions, changing the direction of the gradient can turn a cation selective channel into an anion selective channel.[10] Interestingly, the inversion of selectivity is not restricted to experiments with variable pH: Anionic selectivity was found in experiments with salts of divalent cations at neutral pH[9] and was attributed to specific binding of divalent cations at the channel central constriction.[20] The experiments for 2:1 salts display a correlation between measured reversal potential and calculated bulk diffusion potential. This accord, not found in the case of 1:1 salts, indicates that the measured potential for salts of divalent cations is mostly due to the different mobilities of anions and cations.[9]

Motivated by those results in salts of divalent cations and by the reported evidence that monovalent cations may also bind to some negative residues of the OmpF channel,[13,16,21] we present here a series of experiments aimed to dissect the diverse contributions to the overall measured selectivity and to extract useful information about the way monovalent cations like Li^+, Na^+, K^+, and Cs^+ permeate through the OmpF channel. In a former study, we showed that measured selectivity attains certain saturation with increasing concentration gradient, what we named as "salting out the channel selectivity".[4] Now, the method involves measuring RP at higher concentration ratios, beyond those gradients used in most channel selectivity studies, so that the underlying physical mechanisms could be more easily set

* Corresponding author. E-mail: alcaraza@fca.uji.es. Phone: +34-964-728044. Fax: +34-964-729218.

10.1021/jp902267g CCC: $40.75
Published on Web 06/01/2009

apart. The common pattern observed for the four salts studied in the change of RP with the concentration ratio is rationalized in terms of a simple molecular model that, on the basis of the original study by Hill,[22] calculates the grand canonical partition function of a pair of interacting sites where there is competition between proton association and cation binding. With a minimum of structural details in the model, we get a reasonable qualitative agreement between theory and experiment. A similar combination of macroscopic and microscopic approaches has been useful in the study of related sytems, like the KcsA and MthK potassium channels.[23]

Experimental Section

Reversal Potential Measurements. The experiments reported here have been carried out in single ion channels reconstituted on planar membranes. Lipid bilayers were formed by aposition of two monolayers made from 5 mg/mL solution of diphytanoylphosphatidylcholine (DPhPC) (Avanti polar lipids, Inc., Alabaster, AL) in pentane (Baker) on 70−100 μm diameter orifices in a 15 μm thick Teflon partition that separates two chambers. The orifices where pretreated with 1% solution of hexadecane in pentane. The aqueous solutions of KCl, NaCl, LiCl, and CsCl were buffered by 5 mM Hepes, and the pH was fixed at 6. All measurements were performed on single OmpF channels at room temperature (24.0 ± 1.5 °C). Wild-type OmpF, kindly provided by Dr. Mathias Winterhalter (Jacobs University, Germany), was isolated and purified from an *Escherichia coli* culture. Channel insertion was achieved by adding 1 mg/mL solution of OmpF in the buffer that contained 1 M KCl and 1% (v/v) of OctylPOE (Alexis, Switzerland) to 2 mL of aqueous phase at the *cis* side of the membrane.

The electric potential was applied using Ag/AgCl electrodes in 2 M KCl, 1.5% agarose bridges assembled within standard 250 μL pipet tips. Potential is defined as positive when it is greater at the side of protein addition (the *cis* side of the membrane cell), while the *trans* side is set to ground. An Axopatch 200B amplifier (Molecular Devices, Sunnyvale, CA) in the voltage-clamp mode was used for measuring the current and applying potential. The membrane chamber and the headstage were isolated from external noise sources with a double metal screen (Amuneal Manufacturing Corp., Philadelphia, PA).

The RP was obtained as follows. First, a lipid membrane was formed at a given salt concentration gradient. Second, an OmpF channel was inserted at zero potential and the channel conductance was checked by applying +100 mV/−100 mV. In some experiments, potentials of ∼ −100 mV were applied to accelerate channel insertion. Third, the ionic current was manually set to zero by adjusting the applied potential. The potential needed to achieve zero current, V_{Exp}, was then corrected by the liquid junction potential calculated from Henderson's equation to obtain RP. Details can be found elsewhere.[9] Each point was measured for at least three different experiments to ensure reproducibility and to estimate the standard deviation.

Results and Discussion

Exclusion and Diffusion at High Concentration Gradients. We have measured the OmpF channel RP at pH 6 in a number of salts of monovalent cations: LiCl, NaCl, KCl, and CsCl. The ratio, r, between salt concentrations on both solutions was varied from 3 to 200. The salt concentration on the *trans* solution (electrically grounded) was always 0.03 M in all experiments, whereas the concentration on the *cis* solution (the side of the protein addition) was increased from 0.09 to 6 M (or up to the highest concentration compatible with the salt solubility in water).

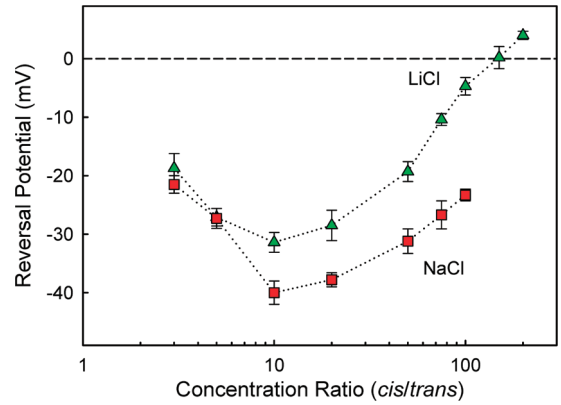

Figure 1. OmpF channel RP measured in LiCl (triangles) and NaCl (squares) at pH 6. The salt concentration is 0.03 M on the *trans* side, and the concentration on the *cis* side varies from 0.09 to 6 M (LiCl) or 3 M (NaCl). The dashed line marks the limit between cationic (negative RP) and anionic (positive RP) channel selectivity under these experimental conditions.

Figure 1 shows the OmpF RP in LiCl and NaCl for increasing concentration ratio $r = c_{cis}/c_{trans}$. None of the two sets of measurements displays the monotonic trend previously reported in experiments with relative low gradients (typically up to $r \approx 20$).[4,9,16] In both electrolytes, the absolute value of the RP increases with the concentration ratio, then reaches a maximum, and later decreases. In terms of selectivity, the channel cationic selectivity increases with the concentration gradient for low ratios but decreases at high ratios. Interestingly, the channel selectivity can be even reversed if the concentration ratio is large enough, as is the case of LiCl in the 6 M|0.03 M experiment. On the one hand, this finding adds new evidence to the reported fact that ion selectivity in large channels is not just a number but strongly depends on experimental conditions.[4] On the other hand, this result can help us to understand better the role of the factors contributing to channel selectivity. Recall that the main mechanisms responsible for monovalent ion selectivity in wide channels are, in principle, electrostatic exclusion, due to interactions between mobile ions and fixed charges, and diffusion, due to differences in ion mobilities.[9]

The simplest approach for estimating the contribution of electrostatic exclusion to RP is given by Donnan formalism,[1,24] and is based on the continuity of the electrochemical potential of each permeating species at the channel/solution interface. In this framework, the electric potential drop due to electrostatic exclusion of co-ions and accumulation of counterions within a negative charged channel in a 1:1 electrolyte can be calculated as follows:

$$\Delta\phi_{exclusion} \equiv \Delta\phi_{Donnan-cis} - \Delta\phi_{Donnan-trans} = \frac{k_B T}{e} \ln \frac{(-X/2c_{trans}) + \sqrt{(-X/2c_{trans})^2 + 1}}{(-X/2c_{cis}) + \sqrt{(-X/2c_{cis})^2 + 1}} \quad (1)$$

where X denotes the channel fixed charge concentration, k_B is Boltzmann's constant, T is the absolute temperature, and e is the elementary charge. For the sake of simplicity, activities are ideally replaced by concentrations. OmpF porin is cationic selective at neutral pH, so under the conditions studied here ($c_{cis} > c_{trans}$) the electric potential difference given by eq 1 is always negative and increases in magnitude with concentration ratio. This is illustrated in the solid line plot of Figure 2. In the present case, c_{trans} is kept constant at a relatively low value, so

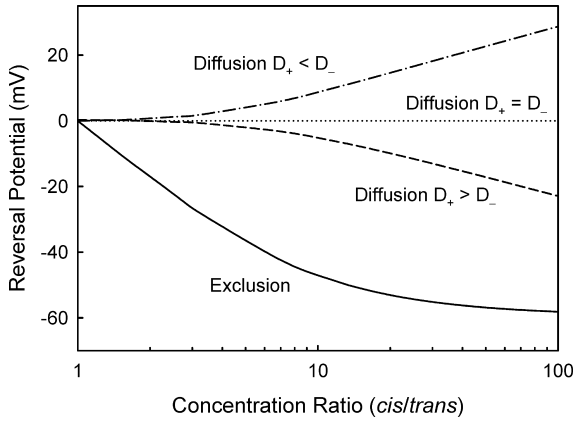

Figure 2. Solid line: Plot of the total Donnan potential drop (exclusion contribution to RP) for a channel with an average negative fixed charge concentration of $X = 0.3$ M. The salt concentration is 0.03 M on the *trans* side, and the concentration on the *cis* side varies from 0.09 to 3 M. Dashed and dotted lines: Diffusion potential across the channel in three different cases of relative cation and anion mobilities as labeled ($D_+ = 0.5D_-$; $D_+ = D_-$; $D_+ = 2D_-$). With the exception of CsCl, all salts explored in our OmpF RP experiments correspond to the case $D_+ < D_-$.

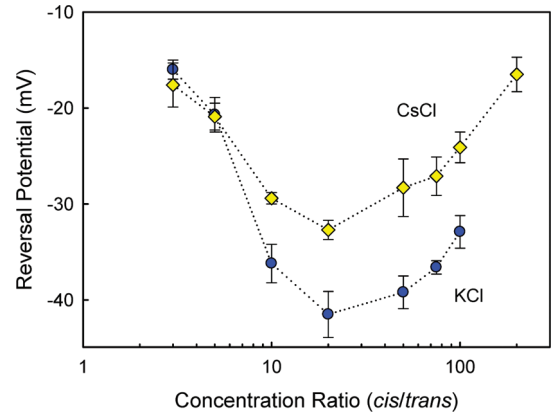

Figure 3. OmpF channel RP measured in CsCl (diamonds) and KCl (circles) at pH 6. The salt concentration is 0.03 M on the *trans* side, and the concentration on the *cis* side varies from 0.09 to 6 M (CsCl) or 3 M (KCl).

that the Donnan potential drop at the *trans* interface remains constant. On the contrary, c_{cis} varies from low to high concentration so that the Donnan potential drop at the *cis* interface decreases with increasing concentration until it practically vanishes when $c_{cis} \gg X$. Then, only the *trans* interface contributes to the total exclusion potential, what explains the observed saturation. The use of an averaged fixed charge concentration X for the whole channel could seem an excessive simplification, since each OmpF porin contains 306 ionizable residues, both positives and negatives. However, previous studies give some credit to the use of average values in OmpF by showing that certain channel features like current−voltage characteristics or ion selectivity at low concentration ratios are mainly regulated by the collective action of a large number of residues rather than by specific interactions at certain particular locations.[7,25,26]

Aside from the exclusion effects (modulated by the salt concentrations on both bulk solutions), the fact that cations and ions generally have different mobilities gives rise to some charge separation quantified by the diffusion potential.[27] The simplest way to estimate it is by using the Planck approximation of electroneutrality along the diffusion region, i.e., the channel. For a binary salt of monovalent ions, Planck's equation for the diffusion potential (following the convention *cis* minus *trans*) reads[24]

$$\Delta\phi_{\text{diffusion}} = \frac{k_B T}{e}\frac{D_- - D_+}{D_- + D_+}\ln\frac{D_+\bar{c}_{cis} + D_-(\bar{c}_{cis} - X)}{D_+\bar{c}_{trans} + D_-(\bar{c}_{trans} - X)} \tag{2a}$$

where

$$\begin{aligned}\bar{c}_{cis} &= c_{cis}\exp[(e/k_B T)\Delta\phi_{\text{Donnan}-cis}]\\ \bar{c}_{trans} &= c_{trans}\exp[(e/k_B T)\Delta\phi_{\text{Donnan}-trans}]\end{aligned} \tag{2b}$$

D_+ and D_- denote the diffusion coefficient of cations and anions, respectively. As in eq 1, activities are replaced by concentrations. $\bar{c}_{cis}$ and $\bar{c}_{trans}$ denote the cation concentrations in the *cis* and *trans* channel interfaces, which differ from bulk concentrations due to the electrostatic exclusion, as indicated in eq 2b. Plots of eq 2a for the conditions studied here ($c_{cis} > c_{trans}$) are also shown in Figure 2 (dashed and dotted lines). The diffusion potential has the same sign as the Donnan potential for $D_+ > D_-$ but the opposite for $D_+ < D_-$. Considering that $D_+ < D_-$ for free solutions of NaCl and LiCl, we expect that in a cation selective channel like OmpF exclusion and diffusion follow opposite trends as the concentration ratio increases. Interestingly, for high enough values of r (e.g., $r > 50$), eq 2a can be written to a good approximation as

$$\Delta\phi_{\text{diffusion}} \approx A + \frac{k_B T}{e}\frac{1 - D_+/D_-}{1 + D_+/D_-}\ln r \tag{2c}$$

where A is independent of r, so that the diffusion potential scales with the logarithm of the bulk concentration ratio (note that c_{trans} and $\bar{c}_{trans}$ are both constant, and when $c_{cis} \gg X$, the Donnan potential at the *cis* channel interface is negligible and $\bar{c}_{cis} \approx c_{cis}$).

By assuming that RP contains both exclusion and diffusion, the RP measurements shown in Figure 1 allow a trivial qualitative explanation: upon increasing salt concentration on the *cis* side, the electrostatic exclusion (solid line in Figure 2) attains almost a *plateau*, whereas the potential drop stemming from the difference between cation and anion mobilities (dotted−dashed line in Figure 2) keeps on growing with the concentration ratio. According to this picture of channel selectivity, the nonmonotonic trends observed in Figure 1 would be a result of the antagonism between exclusion and diffusion.

To get further insight on the relative roles of diffusion and exclusion, we performed RP experiments in KCl and CsCl, shown in Figure 3. What makes these two salts different from the other two mentioned before is that K^+ and Cs^+ have almost the same bulk mobility as Cl^-, so that the role of diffusion in RP should be nearly identical for both salts and considerably less significant than in NaCl and LiCl. However, this is not the case: The measured points resemble those shown in Figure 1, suggesting that in both cases cations diffuse considerably more slowly than anions. This is especially intriguing in the case of CsCl, since $D_{Cs} > D_{Cl}$ in free solution, which would be consistent with a small but negative slope of RP vs ln r at high ratios. In addition, Figure 3 shows also a significant difference in RP (ca. 10 mV) between KCl and CsCl at high concentration ratios. Considering that K^+ and Cs^+ have the same electrical charge

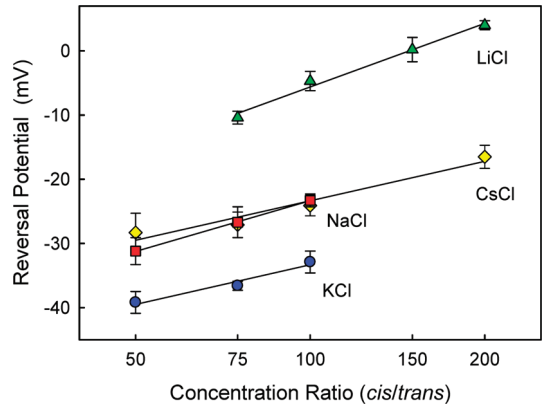

Figure 4. Logarithmic plot of the RP change with the concentration ratio. For CsCl (diamonds), KCl (circles), and NaCl (squares), the linear fit of RP vs ln r includes measurements at $r \geq 50$. For LiCl (triangles), fitting involves data taken at $r \geq 75$. The pH was kept at 6. The salt concentration on the *trans* side was fixed at 0.03 M. The salt concentration on the *cis* side was increased from 1.5 to 6 M (3 M in the KCl and NaCl series).

and very close bulk diffusivities, we can hypothesize then that there is an additional physicochemical phenomenon, not included in eqs 1 and 2a, that exerts a crucial effect on ion selectivity in the OmpF channel. This subtle phenomenon has slipped by in many of the theoretical approaches describing ion transport through the OmpF channel, both in continuum models based on Nernst−Planck equations[4,7] and in computational MD simulations.[14,15,28]

Interestingly, a pioneer study based on fluorescence experiments pointed to the existence of a binding site for monovalent cations in the OmpF channel, with a reported dissociation constant for Na^+ in the millimolar range.[21] More recently, MD simulations and free-energy calculations came to a similar conclusion and even located this binding site for cations in the central narrow constriction of the channel near the aspartic acid residue D113.[13,16] It is important to note that in such a scenario the cations do not block the wide OmpF porin, as would be the case of a narrow channel where single-file transport takes place. Instead of this, a "push-out" mechanism similar to an ion-exchange reaction that effectively slows down the permeation of cations is more plausible.[13] Extensive studies with wild-type OmpF and its mutants,[29,30] together with conductance experiments and noise analysis in wild-type OmpF,[19,31] indicate that another acidic residue, the glutamic acid E117, is probably involved as well in the binding phenomenon. The physiological relevance of this site is still poorly understood but appears to be essential for certain particular channel features like the strong dependence of conductance on pH,[19,31,32] the fact that cations and anions follow well-separated permeation pathways along the OmpF porin,[14,15] or the translocation of certain antibiotics across the channel.[33,34] The question arising now is whether a more detailed analysis of the RP measurements shown in Figures 1 and 3 can add support to this hypothetical cation binding in the OmpF channel.

Let us focus our attention to RP measurements for high concentration ratios. Figure 4 shows that a common pattern can be found for all four electrolytes studied (KCl, NaCl, LiCl, CsCl). For r above 50, the measured RP scales rather well with the logarithm of the *cis*/*trans* concentration ratio. Having in mind the discussion of Figure 2, this fact has two major implications. On the one side, it indicates that for high concentration ratios ion transport has a predominant diffusional nature. On the other side, it suggests that electrostatic exclusion attains actually certain saturation (this means $\bar{c}_{cis} \approx c_{cis}$), because a hypothetical change in the effective fixed charge of the channel with r would have distorted the correlation found between RP and ln r. Solid lines correspond to the least-squares fittings of experimental data by using eq 2c as model. The ratio D_+/D_- is the only fitting parameter. The best fit values for each electrolyte are shown in Table 1.

The comparison between theoretical slopes (calculated using bulk diffusion coefficients in eq 2c) and experimental slopes of RP vs ln r indicates that ion−channel interactions transform radically the electrolyte diffusivities, minimizing their differences so that they effectively perform similarly (see values of the effective ratio $(D_+/D_-)_{eff}$ in Table 1). Interestingly, when the ratios $(D_+/D_-)_{eff}$ are compared to the bulk ones, $(D_+/D_-)_{bulk}$, we find that the diffusivity ratios in the channel are approximately half of their bulk values for all alkali metal cations studied here. If this phenomenon is tentatively attributed to the binding site for cations commented before, it is important to note that the binding constant given by the literature, K_d, is in the millimolar range,[21] a relatively small concentration. This means that at the (high enough) salt concentrations here explored the binding sites would be saturated for all of the cations and the binding mechanism would have the same effect for all of the cations. This would explain, intuitively, why all of the ratios are reduced in the same proportion. Despite whether this conjecture could seem reasonable or not, a deeper analysis seems mandatory.

Modeling the Effect of Cation Binding on Its Relative Diffusivity to Anions. The combination of theoretical approaches (MD simulations, free-energy calculations[13,16]) and experimental techniques like fluorescence, electrophysiology, mutagenesis, and noise analysis[19,21,29−31] provides evidence for the existence of a binding site for cations in the OmpF channel. This phenomenon is not due to the collective action of a large number or residues but, on the contrary, is specifically linked to certain acidic residues located in the central channel constriction. Thus, a different level of approximation that the sole use of continuum theories invoking averages seems desirable. To this end, we have considered the effect of a binding site on the basis of the statistical mechanics formalism developed by T. L. Hill[22] for matching pairs of interacting sites. Mafé and coworkers used a similar model to study the binding of antibiotic molecules to the OmpF porin[34] and the pK_a shifts in weak polyacids.[35] This approach has the benefit of simplicity on completion of introducing a reduced number of structural details. Thus, other factors like conformational changes, solvent effects, and the particular nature of the aminoacid hydrocarbon chain[36,37] are not considered here. As mentioned above, previous studies link the binding site for cations to the acidic residues D113 and E117, located in the narrow central constriction of the OmpF channel.[13,16] Single-channel current noise experiments have revealed that the low-frequency spectral density has a pronounced peak at a pH considerably lower than the tabulated values for aspartic and glutamic acid, and interestingly, the position of the peak depends crucially on the electrolyte concentration.[19] This suggests that cations compete with protons to effectively titrate the negative residues D113 and E117. To obtain the relevant equations, we consider each pair of sites as a system in a grand canonical ensemble.[22,34,35] The states for hydrogen and salt cation occupation are symbolically represented in Figure 5, together with their respective contribution to the grand partition function (for the sake of clarity, we have considered a potassium ion, but the formalism can be applied to any monovalent cation). Having in mind that the tabulated

TABLE 1: Theoretical Slope of Diffusion Potential (eq 2c) and Experimental Slope of RP vs ln *r* for Alkali Metal Salts in the OmpF Channel

salt	CsCl	KCl	NaCl	LiCl
theoretical slope	−0.19	0.45	5.3	8.3
experimental slope[a]	8.9 ± 1.3	8.9 ± 1.8	11.4 ± 0.1	14.3 ± 0.8
$(D_+/D_-)_{eff}$	0.48 ± 0.06	0.48 ± 0.08	0.38 ± 0.01	0.28 ± 0.03
$(D_+/D_-)_{eff}/(D_+/D_-)_{bulk}$	0.48 ± 0.06	0.50 ± 0.08	0.58 ± 0.01	0.56 ± 0.05

[a] The measurements of RP were done at pH 6 and a fixed *trans* concentration of 0.03 M. The concentration ratios for CsCl, KCl, and NaCl are higher than 50. For LiCl, the concentration ratios are greater than 75.

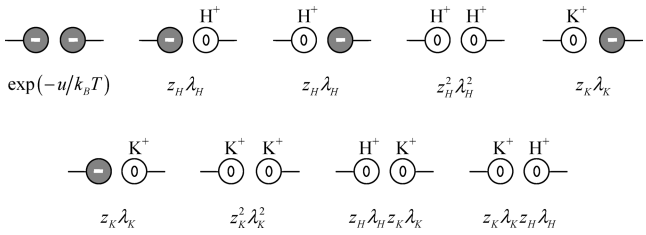

Figure 5. States for hydrogen and potassium occupation of the two acid groups together with the respective contributions to the grand partition function.

free solution pK_a's of aspartic and glutamic acid are, respectively, 4.0 and 4.1,[38] it seems reasonable to treat them as identical interacting sites. Note that although the model introduces an effective binding constant for the ion pair formed by the salt cation and the acidic residue, no particular molecular mechanism is invoked for this pairing. No Debye screening is considered, because the distance between charged groups is too small (several angstroms). However, the model assumes implicitly that the proximity of the cation or the proton to the oppositely charged residue effectively screens this charge.[34] Thus, increasing salt concentration contributes to the neutralization of acid residues and then the apparent pK_a of the weak acid could be significantly decreased, as observed in current noise experiments.[19]

According to this formalism, the matching charge states (nonexistent in the present case) are energetically favored, whereas the states with charges of the same sign are energetically discouraged.[35] The nine states shown in Figure 5 can be averaged to obtain the properties of the system using the statistical thermodynamics formalism of the partition function.[22,36] Following Hill's approach, z_i in Figure 5 are the partition functions of ion i bound to the site and λ_H and λ_K are magnitudes proportional to the absolute activities of the hydrogen and the salt cation, respectively, defined as $z_H\lambda_H = 10^{pK_a-pH}$ and $z_K\lambda_K = 10^{pK_c}c$, with K_c being the cation binding constant and c the KCl concentration in M units. Thus, the grand partition function for this case is

$$\begin{aligned} q &= \exp(-u/k_BT) + 2z_H\lambda_H + 2z_K\lambda_K + 2z_H\lambda_H z_K\lambda_K + \\ &\quad z_H{}^2\lambda_H{}^2 + z_K{}^2\lambda_K{}^2 \\ &= \exp(-u/k_BT) + 2(10^{pK_a-pH}) + 2(10^{pK_c}c) + \\ &\quad 2(10^{pK_a-pH}10^{pK_c}c) + 10^{2(pK_a-pH)} + (10^{pK_c}c)^2 \end{aligned} \quad (3)$$

The fraction, x, of free acid (without any K^+ bound) can be calculated from the grand partition function of the system q as $(1 - x) = (1/2)\lambda_K(\partial \ln q/\partial\lambda_K)$, so that x is given by

$$\begin{aligned} x = \frac{1}{q}[&\exp(-u/k_BT) + 2(10^{pK_a-pH}) + 10^{pK_c}c + \\ &10^{pK_a-pH}10^{pK_c}c + 10^{2(pK_a-pH)}] \end{aligned} \quad (4)$$

The present study is restricted to neutral conditions (pH 6) when both acidic residues are deprotonated and terms containing $z_H\lambda_H$ are not principal. However, when the pH is lowered, the competition between proton association and cation binding becomes apparent and the fraction α of protonated acid can be calculated using λ_H instead of λ_K, i.e., $(1 - \alpha) = (1/2)\lambda_H(\partial \ln q/\partial\lambda_H)$ as a function of pH, giving reason for the observed pK_a shift of channel acidic residues.[19,32] In addition, note that for typical values of the interaction energy, u, between ionized negative residues (∼3−4 k_BT) the term $\exp(-u/k_BT)$ can be neglected when compared to the main contribution to x.

Once the fraction of groups affected by the binding is calculated at a certain concentration, we can wonder how the cation binding site affects the ion transport across the channel. To get a rough qualitative answer, we consider that the effective diffusion coefficient of the permeating cations, D_{eff}, is a weighted average of D_{free}, the cation diffusion coefficient in the absence of binding, and D_{bound}, the diffusion coefficient of cations in a channel where the cation binding site is always occupied. By using the fraction of free acid, x, as a weighing factor, we get[39,40]

$$D_{eff} = xD_{free} + (1 - x)D_{bound} \quad (5)$$

The values for D_{free} can be taken from the literature.[1] The question that arises naturally is which values should be used then for D_{bound}. Recall that OmpF is a wide channel allowing multiionic transport, and the existence of a binding site does not imply the channel blocking (where one could expect $D_{bound} \approx 0$) but a hindered cation electrodiffusion.[13] The reduction of the diffusion coefficient of a particle caused by a binding site has been reported both experimentally and theoretically.[41] Looking back to Figure 4 and Table 1, at high concentration ratio, we can find a common pattern for all alkali metal cations under study: the diffusivity ratios in the channel are approximately half of their bulk values. If we consider that in Figure 4 the concentration is high enough to ensure that the fraction of free acid groups is close to zero, we can identify this effective diffusion coefficient with $D_{bound} \approx D_{free}/2$. This value seems reasonable in the light of MD simulations performed by Suenaga and collaborators that suggest a "push-out" transport mechanism involving simultaneously two cations. According to their simulation, cation 1 moved slowly through the pore until it formed the ion pairing with D113 for a certain time. Cation 2 moved through the pore in a similar way and pushed out cation 1, so that cation 2 formed the ion pairing with D113. This process is an ion exchange reaction, and the total result is that a single cation takes about 1.3 ns to cross the channel and approximately half of this time is involved in ion-pairing interactions.[13] The particular cation−acid chemistry could modify those interactions and explain the small differences found between the alkali metal cations employed.

Figure 6 shows both the calculated fraction of free sites and the effective diffusion coefficient of cations as a function of electrolyte concentration, for several values of pK_c. The reasons why several

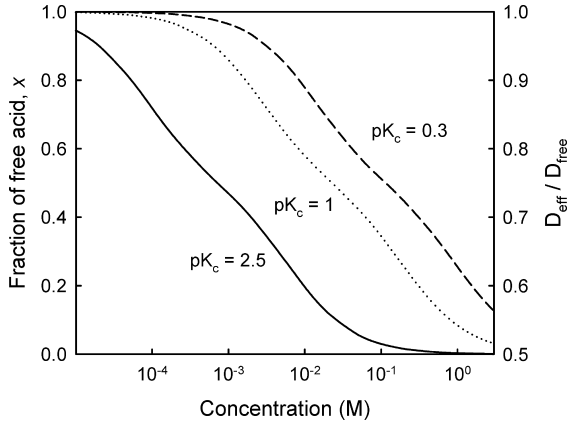

Figure 6. Model calculation of the fraction of free sites (left axis) and the effective diffusion coefficient of cations (right axis, normalized to free solution values) as a function of salt concentration, for several values of pK_c as labeled.

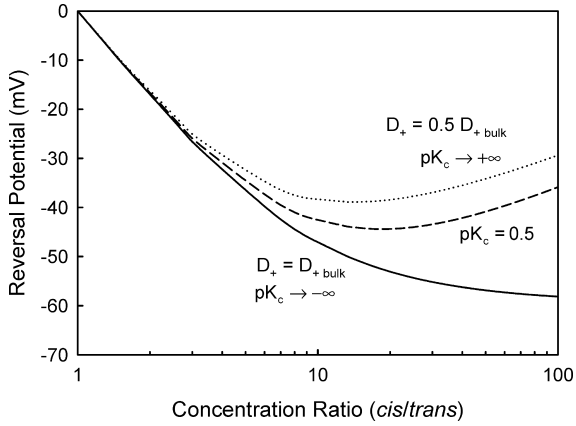

Figure 7. Calculated RP as a function concentration ratio, *r*. The salt concentration on the *trans* side was fixed at 0.03 M. The salt concentration on the *cis* side was increased up to 3 M.

values are presented are the following: Carboxylic aminoacids have been considered as relatively strong cation coordinating residues in the literature.[34] Dissociation constants of alkaline ions bound to carboxylic groups can be found in a wide range of values, from 0.01−1 M in macromolecules to 0.5−10 M in acidic lipid membranes. In the OmpF channel, fluorescence experiments yield a dissociation constant of 3 mM for Na^+, which means p$K_c \approx 2.5$. However, because of the cation accumulation inside the channel induced by the overall negative fixed charge, the corresponding cation concentration in the vicinity of the binding site should be much higher than 3 mM. Simple considerations following electroneutrality condition suggest that the concentration of counterions must be comparable to the fixed charge concentration, which is around 0.3 M.[4,7] Thus, a concentration of 3 mM in the bathing solution could actually mean a local concentration near the binding site around 0.3 M (p$K_c \approx 0.5$). Anyway, the trend shown in Figure 6 is clear; the lower the pK_c, the higher the ionic concentration needed to obtain a significant amount of bound cations that slow down the effective cation diffusion coefficient, D_{eff}.

Once the effect of the binding site on the cation diffusivity is tentatively described, we can analyze how RP changes when cation diffusion coefficient D_{free} is replaced by D_{eff} in eq 2a. With D_{eff} being a weighted average between D_{free} and $D_{free}/2$, it is evident that the RP calculated using D_{eff} will be enclosed between these two limiting cases. Figure 7 shows the OmpF RP in KCl calculated by adding up the contributions given by eq 1 (Donnan exclusion) and eq 2a (diffusion with D_{eff} instead of D_{free}). The model RP is a

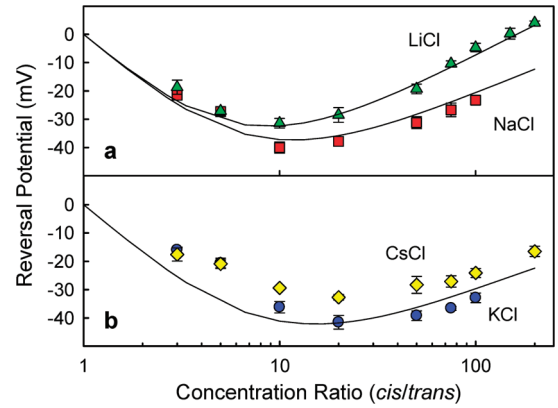

Figure 8. Symbols: OmpF RP measured at pH 6 in LiCl (triangles), NaCl (squares), CsCl (diamonds), and KCl (circles). The salt concentration is 0.03 M on the *trans* side. Lines: Model calculations of RP ($X =$ 0.3 M and p$K_c = 0.5$).

monotonic function of the concentration ratio when bulk values are used for the diffusivities. In contrast, RP turns into a nonmonotonic function once the effect of the cation binding on the ion diffusivity is computed using a plausible value for binding constant of p$K_c \approx 0.5$.

Up to this point, we have shown how a cation binding could reasonably regulate the diffusional transport in the channel giving rise to nonmonotonic RP as displayed by Figures 1 and 3. However, a direct comparison between theory and experiments is required. Figure 8a shows RP measurements in NaCl and LiCl together with the theoretical results (solid lines). Due to the diversity of physicochemical phenomena involved, no attempt of a quantitative fitting has been made. Electrostatic exclusion has been calculated using eq 1, and an average value of $X \approx 0.3$ M was found in agreement with previous approaches.[4,7] Diffusion has been calculated by using tabulated bulk diffusivities for each electrolyte but replacing in each case D_{free} by the effective one, D_{eff}, obtained from a binding constant of p$K_c \approx 0.5$.

The qualitative agreement found between theory and experiment is reasonable if one takes into account the wide range of concentration ratios explored, the variety of salts, and the lack of structural details of the model. Both X and pK_c values have been taken from the literature, as mentioned above. However, fine-tuning of the model could be done by taking into account the specificity of each cation in the interaction with the channel binding residues. Thus, pK_c could differ from Na^+ to Li^+. From the inspection of Figure 8a, one could expect a better agreement between theory and experiments if p$K_c > 0.5$ for LiCl (triangles) and p$K_c < 0.5$ for NaCl (squares). That would be consistent with a scenario where the smaller cation Li^+ binds more easily than the larger Na^+. However, the RP calculations shown in Figure 8b seem to contradict such a trivial explanation. RP measurements in KCl and CsCl are shown together with the model predictions (the two solid lines are superimposed). We have used the same parameters as in Figure 8a, except for the bulk diffusivities for Cs^+ and K^+, taken from the literature (note that they differ by less than 5%).

Again, a good qualitative agreement is found between theory and experiment. In the present case, a better accord could be found using p$K_c > 0.5$ in the case of CsCl and p$K_c < 0.5$ in the case of KCl. However, this would mean that the larger Cs^+ binds more easily than the smaller K^+. Definitely, ion size is not the sole determinant of the particular cation−residue chemistry and other factors like hydration energies could play a significant role. That is the reason why quantitative fittings make little sense here. There is no point in speculating about

the actual values of pK_c when reliable values of the fixed charge concentration and ion diffusivities are unknown.

To sum up, the comparison of RP measurements at high concentration ratios in different monovalent salts suggests that the selectivity of the OmpF channel cannot be understood only in terms of electrostatic exclusion and diffusion. An additional phenomenon, a binding of cations to certain acidic channel residues, is likely to be also involved, and its contribution is essential to account for the observed channel features. A simple molecular model provides qualitative explanations to some of the observed phenomena and can be useful for future more elaborated treatments, especially all-atom MD simulations.[42]

Conclusions

We have studied the ionic selectivity of the bacterial porin OmpF in several monovalent alkali metal salts. Our results show that RP measurements performed at large concentration ratios can provide useful information about the mechanisms contributing to the channel selectivity. In particular, the experimental data reveal that for high enough concentration gradients cation diffusion is hampered in a similar way for the four salts explored (LiCl, NaCl, CsCl, and KCl). This is consistent with the reported existence of a binding site for cations at the channel central constriction. On the basis of this evidence, we present a simple molecular model for the binding interaction between cations and two acidic residues with a minimum amount of structural information. Despite its simplicity, this model, combined with Donnan formalism for electrostatic exclusion and Planck's expression for diffusion within the channel, accounts qualitatively for the reduction of OmpF cation selectivity at large gradients. The main findings can be summarized as follows:

(i) In contrast to what it is generally accepted, the channel cationic selectivity is not a monotonic function of the concentration ratio but, after reaching a maximum, decreases with the increasing gradient and can even be reversed as in the case of LiCl.

(ii) The channel RP is dominated by the contribution of the diffusion potential at high enough concentration ratios, evidence that electrostatic exclusion (accumulation) of anions (cations) attains certain saturation.

(ii) There is a common pattern in the reduction (~50%) of the ratio between cation and anion diffusion coefficients within the channel for the four salts studied, compared to bulk values.

(iv) This hampered diffusion is consistent with the reported existence of a cation binding site at the channel central constriction, near two acidic residues with similar ionization properties.

(v) By using data taken from the literature for the average channel fixed charge concentration and the binding constant of cations in the OmpF channel, we get a reasonable qualitative agreement between theory and experiment.

Acknowledgment. The authors acknowledge support from the Spanish Ministry of Education (project FIS2007-60205). We are grateful to Prof. Salvador Mafé for stimulating discussions and reading parts of the manuscript.

Supporting Information Available: A sample of current−voltage curves measured in NaCl and LiCl, showing that even at high concentration gradients the channel exhibits ohmic behavior. This material is available free of charge via the Internet at http://pubs.acs.org.

References and Notes

(1) Hille, B. *Ion channels of excitable membranes*; Sinauer: Sunderland, MA, 2001.

(2) Kuyucak, S.; Andersen, O. S.; Chung, S.-H. *Rep. Prog. Phys.* **2001**, *64*, 1427–1472.

(3) Roux, B.; Allen, T.; Bernèche, S.; Im, W. *Q. Rev. Biophys.* **2004**, *37*, 15–103.

(4) Alcaraz, A.; Nestorovich, E. M.; Aguilella-Arzo, M.; Aguilella, V. M.; Bezrukov, S. M. *Biophys. J.* **2004**, *87*, 943–957.

(5) Alcaraz, A.; Ramírez, P.; García-Giménez, E.; López, M. L.; Andrio, A.; Aguilella, V. M. *J. Phys. Chem. B* **2006**, *110*, 21205–21209.

(6) Ramírez, P.; Aguilella-Arzo, M.; Alcaraz, A.; Cervera, J.; Aguilella, V. M. *Cell Biochem. Biophys.* **2006**, *44*, 287–312.

(7) Aguilella-Arzo, M.; García-Celma, J. J.; Cervera, J.; Alcaraz, A.; Aguilella, V. M. *Bioelectrochemistry* **2007**, *77*, 320–327.

(8) Aguilella-Arzo, M.; Andrio, A.; Aguilella, V. M.; Alcaraz, A. *Phys. Chem. Chem. Phys.* **2009**, *11*, 358–365.

(9) Alcaraz, A.; Nestorovich, E. M.; López, M. L.; García-Giménez, E.; Aguilella, V. M.; Bezrukov, S. M. *Biophys. J.* **2009**, *96*, 56–66.

(10) García-Giménez, E.; Alcaraz, A.; Aguilella, V. M.; Ramírez, P. *J. Membr. Sci.* **2009**, *331*, 137–142.

(11) Nikaido, H. *Microbiol. Mol. Biol. Rev.* **2003**, *67*, 593–656.

(12) Delcour, A. H. *Front. Biosci.* **2003**, *8*, d1055-d1071.

(13) Suenaga, A.; Komeiji, Y.; Uebayasi, M.; Meguro, T.; Saito, M.; Yamato, I. *Biosci. Rep.* **1998**, *18*, 39–47.

(14) Im, W.; Roux, B. *J. Mol. Biol.* **2002**, *319*, 1177–1197.

(15) Im, W.; Roux, B. *J. Mol. Biol.* **2002**, *322*, 851–869.

(16) Danelon, C.; Suenaga, A.; Winterhalter, M.; Yamato, I. *Biophys. Chem.* **2003**, *104*, 591–603.

(17) Gillespie, D.; Eisenberg, R. S. *Eur. Biophys. J.* **2002**, *31*, 454–466.

(18) Barry, P. H. *Cell Biochem. Biophys.* **2006**, *46*, 143–154.

(19) Nestorovich, E. M.; Rostovtseva, T. K.; Bezrukov, S. M. *Biophys. J.* **2003**, *85*, 3718–3729.

(20) Yamashita, E. M.; Zhalnina, V.; Zakharov, S. D.; Sharma, O.; Cramer, W. A. *EMBO J.* **2008**, *27*, 2171–2180.

(21) Kobayashi, Y.; Nakae, T. *Eur. J. Biochem.* **1985**, *151*, 231–236.

(22) Hill, T. L. *J. Am. Chem. Soc.* **1956**, *78*, 3330–3336.

(23) Nimigean, C. N.; Chappie, J. S.; Miller, C. *Biochemistry* **2003**, *42*, 9263–9268.

(24) Lakshminarayanaiah, N. *Equations of Membrane Biophysics*; Academic Press: New York, 1984.

(25) Miedema, H.; Meter-Arkema, A.; Wierenga, J.; Tang, J.; Eisenberg, B.; Nonner, W.; Hektor, H.; Gillespie, D.; Meijberg., W. *Biophys. J.* **2004**, *87*, 3137–3147.

(26) Miedema, H.; Vrouenraets, M.; Wierenga, J.; Gillespie, D.; Eisenberg, B.; Meijberg, W.; Nonner., B. *Biophys. J.* **2006**, *91*, 4392–4400.

(27) Mafé, S.; Pellicer, J.; Aguilella, V. M. *J. Phys. Chem.* **1986**, *90*, 6045–6050.

(28) Tieleman, D. P.; Berendsen, H. J. C. *Biophys. J.* **1998**, *74*, 2786–2801.

(29) Saint, N.; Lou, K.-L.; Widmer, C.; Luckey, M.; Schirmer, T.; Rosenbusch, J. P. *J. Biol. Chem.* **1996**, *271*, 20676–20680.

(30) Phale, P. S.; Philippsen, A.; Widmer, C.; Phale, V. P.; Rosenbusch, J. P.; Schirmer, T. *Biochemistry* **2001**, *40*, 6319–6325.

(31) Asandei, A.; Mereuta, L.; Luchian, T. *Biophys. Chem.* **2008**, *135*, 32–40.

(32) García-Giménez, E.; Aguilella, V. M.; Alcaraz, A. *Biophys. J.* **2009**, Supplement, 602a, Abstract, 3108-Pos.

(33) Nestorovich, E. M.; Danelon, C.; Winterhalter, M.; Bezrukov, S. M. *Proc. Natl. Acad. Sci. U.S.A.* **2002**, *99*, 9789–9794.

(34) Mafé, S.; Ramírez, P.; Alcaraz, A. *J. Chem. Phys.* **2003**, *119*, 8097–8102.

(35) Mafé, S.; García-Morales, V.; Ramírez, P. *Chem. Phys.* **2004**, *296*, 29–35.

(36) Ben-Naim, A. *Statistical thermodynamics for chemistry and biochemistry*; Plenum: New York, 1992.

(37) Ben-Naim, A. *Cooperativity and regulation in biochemical processes*; Kluwer Academic/Plenum: New York, 2001.

(38) Mathews, C. K.; van Holde, K. E. *Biochemistry*; Benjamin/Cummings Pub.: Redwood, CA, 1996.

(39) Liu, M.; Nicholson, J. K.; Lindon, J. C. *Anal. Commun.* **1997**, *34*, 225–228.

(40) Han, S.-H. *Constr. Build. Mat.* **2007**, *21*, 370–378.

(41) Saxton, M. J. *Biophys. J.* **1996**, *70*, 1250–1262.

(42) Chimerel, C.; Movileanu, L.; Pezeshki, S.; Winterhalter, M.; Kleinekathofer, U. *Eur. Biophys. J.* **2008**, *38*, 121–125.

JP902267G